

SIMULATION OF SPONTANEOUS IGNITION IN POROUS MEDIA

P. CASTAÑEDA, D. MARCHESIN, AND J. BRUINING

ABSTRACT. We study the stability of combustion in a porous medium in a simplified model that takes into account the balance between heat generation and heat losses. The temperature dependence of heat generation is given by Arrhenius law. Heat losses are due to conduction to the rock formation. The system evolution is described by an infinite number of nonlinear modes. We show that its long time behavior is dictated by the two dominant modes, whose phase diagram contains two attractors and a saddle, justifying the picture in classical chemical engineering.

1. INTRODUCTION

Combustion *in-situ* is an important methodology to extract heavy oil from reservoirs, provided ignition is sustained and controlled. The geometrical setting of the reaction location and of conductive heat losses is a very important matter. When heat losses become equal to a small reaction heat rate, the system remains trapped in a slow reaction mode; such a mode is indistinguishable from extinction. On the other hand, if heat losses are smaller than the heat generated by the reaction, the temperature and the heat losses will increase, so we expect that the system reaches an equilibrium in a fast reaction mode; this is ignition. Heat losses are strongly dependent on the geometry of the heat generating region. In this article we will only discuss the one-dimensional case, however work in progress includes other geometries.

In Sec. 2 we construct the reactor model that we will study in this work and nondimensionalize it to enter, in Sec. 3, in linear analysis of its equilibria. These steady-state solutions will guide some of the numerical analysis made in Sec. 4. Finally, in Sec. 5 we summarize our results.

2. THE REACTOR MODEL FOR ONE DIMENSIONAL HEAT FLOW

We derive a set of equations that describe the conservation of energy in a porous medium where thermal flow occurs. Fick's law describes the transport of energy by conduction, and Arrhenius' law describes the rate of energy generated by the reaction between oxygen and coke. Then the variation of heat in the domain is equal to that reaction governed by Arrhenius' law inside the domain plus Fick's law, which involves the boundary. For a general domain Ω we have:

$$\frac{d}{dt} \int_{\Omega} Q dV = \int_{\Omega} \Delta H c_o c_c A \exp\left(-\frac{E}{RT}\right) dV + \int_{\partial\Omega} \kappa \nabla T \cdot \hat{n} dS, \quad (1)$$

where $Q = Q(x, t)$ is the thermal energy density, ΔH denotes the reaction enthalpy per unit mass of oxygen, c_o is the concentration of oxygen in the injected gas, c_c is the concentration of carbon (the "fuel") in the porous media, A is the pre-exponential factor, E is the activation energy, and κ denotes the thermal conductivity.

Key words and phrases. 30° CILAMCE, Chemical reactor, Porous media, *In-situ* combustion, Geometrical setting, Heat losses.

In the one dimensional case, the domain in x stretches from 0 to L , and the reaction takes place in the subinterval from zero to a fixed $a < L$. We assume that the thermal conductivity in the interval $x \in [0, a)$ is much larger than in the region $x \in (a, L]$. Thus we can take temperatures uniform in space for the reacting interval, and we can simplify the governing equation.

Notice also, that in the interval $x \in (a, L]$, there is no reaction taking place, there is only heat conduction, $c_o = 0$ there, so Eq. (1) leads to the classical heat equation. In this way, the 1D equations are:

$$\begin{aligned} \rho_e c_e \frac{\partial T}{\partial t} &= \kappa \frac{\partial^2 T}{\partial x^2} & x \in (a, L) \\ \rho_i c_i \frac{\partial T}{\partial t} \Big|_{x=a+} &= \Delta H c_o A \exp\left(-\frac{E}{RT}\right) \Big|_{x=a+} + \frac{\kappa}{a} \frac{\partial T}{\partial x} \Big|_{x=a+} & x \in [0, a]. \end{aligned} \quad (2)$$

We nondimensionalize with

$$x := a\tilde{x}, \quad t := t_R \tilde{t}, \quad \theta := TR/E, \quad L := a\tilde{L}, \quad (3)$$

obtaining

$$\begin{aligned} \frac{\rho_e c_e a^2}{\kappa t_R} \frac{\partial \theta}{\partial \tilde{t}} &= \frac{\partial^2 \theta}{\partial \tilde{x}^2} & \tilde{x} \in (1, \tilde{L}) \\ \frac{\rho_i c_i a^2}{\kappa t_R} \frac{\partial \theta}{\partial \tilde{t}} \Big|_{\tilde{x}=1+} &= \frac{\Delta H c_o c_c A a^2 R}{\kappa E} \exp\left(-\frac{1}{\theta}\right) \Big|_{\tilde{x}=1+} + \frac{\partial \theta}{\partial \tilde{x}} \Big|_{\tilde{x}=1+} & \tilde{x} \in [0, 1]. \end{aligned} \quad (4)$$

Introducing

$$t_R = \frac{\rho_i c_i a^2}{\kappa}, \quad \mathcal{E} = \frac{\rho_e c_e}{\rho_i c_i} \quad \text{and} \quad \gamma = \frac{\Delta H c_o c_c A a^2 R}{\kappa E}, \quad (5)$$

and dropping the tildes, we rewrite the system in the form:

$$\begin{cases} \mathcal{E} \frac{\partial \theta}{\partial t} = \frac{\partial^2 \theta}{\partial x^2} & x \in (1, L), t > 0 \\ \frac{\partial \theta}{\partial t} \Big|_{x=1} = \gamma \exp\left(-\frac{1}{\theta}\right) \Big|_{x=1} + \frac{\partial \theta}{\partial x} \Big|_{x=1+} & x = 1, t > 0 \\ \theta(L, t) = \theta_L & t > 0 \\ \theta(x, 0) = \theta_i(x) & x \in [0, L] \\ \theta(x, t) = \theta(1, t) & x \in [0, 1]. \end{cases} \quad (6)$$

Clearly, any solution of the PDE (6) is always constant in $x \in [0, 1]$. Taking this fact into account, we can perform the analysis either in $[0, L]$ or in $[1, L]$.

As we will see, there are two types of solutions for (6) as far as \mathcal{E} is concerned. The first one corresponds to $\mathcal{E} = 0$ and the second one to $\mathcal{E} > 0$. The first one corresponds to $\rho_e c_e \ll \rho_i c_i$; in the second one, the precise value of \mathcal{E} is irrelevant. Following data for chemical compounds in the work of Tyler (1985) and by Abu-Khamsin *et al.* (1988), we see that $\gamma = 7.0 \times 10^8$.

3. LINEAR STABILITY OF EQUILIBRIA IN THE REACTOR MODEL

The steady-states ϱ are solutions of system (6) that satisfy

$$\begin{cases} \frac{\partial^2 \varrho}{\partial x^2} = 0 & x \in (1, L) \\ \gamma \exp\left(-\frac{1}{\varrho}\right)\Big|_{x=1} + \frac{\partial \varrho}{\partial x}\Big|_{x=1+} = 0 & x \leq 1, \end{cases} \quad (7)$$

with boundary condition $\varrho(L) = \theta_L$ at the right, where θ_L is a non-negative temperature. Then, we look for a similar boundary condition at the left, say $\varrho(1) = \theta_o$, where even if θ_o is unknown, it represents a non-negative temperature.

Clearly the solution of Eq. (7.a) for such Dirichlet BCs is given by the continuous solution

$$\varrho(x) = \begin{cases} \theta_o & x < 1 \\ (\theta_o - \theta_L)r(x) + \theta_L & x \in [1, L], \end{cases} \quad (8)$$

$$\text{with } r(x) := (L - x)/d, \quad x \in [1, L] \quad \text{and} \quad d := L - 1. \quad (9)$$

3.1. Finding the equilibria. Substituting the second equation from (8) into the Eq. (7.b) leads to

$$\gamma d = \Xi(\theta_o), \quad \text{where} \quad \Xi(\theta) := \frac{\theta - \theta_L}{\exp(-1/\theta)}. \quad (10)$$

Therefore L , θ_o , θ_L and γ are intimately related in steady-states. Equation (10) is the same expressions found in (Bruining *et al.*, 2008) and means that we are interested in values $\theta_o > \theta_L$.

Looking for the extrema of the function Ξ , we see that

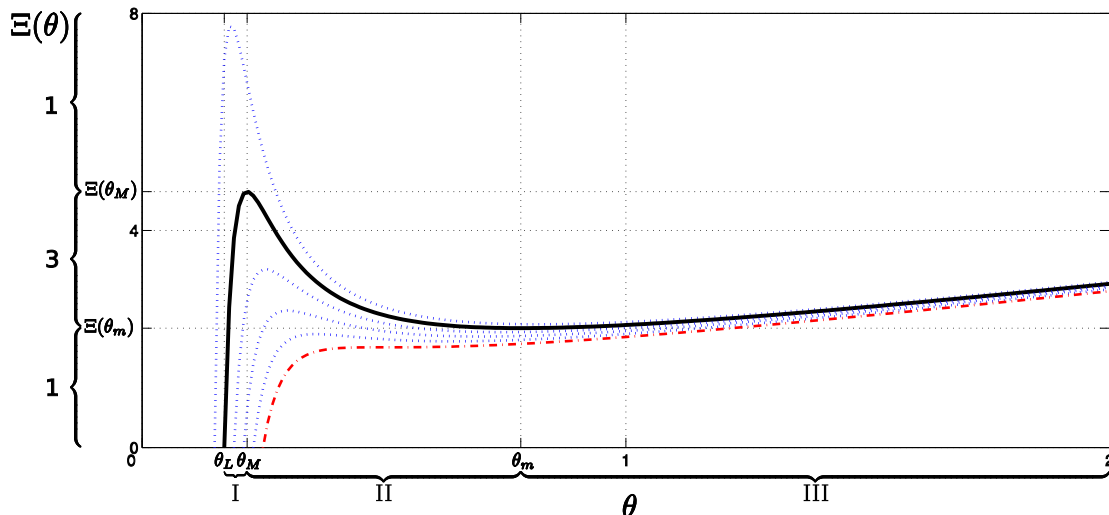
$$\Xi'(\theta) = \frac{d}{d\theta} \left[(\theta - \theta_L) \exp\left(\frac{1}{\theta}\right) \right] = \frac{\theta^2 - \theta + \theta_L}{\theta^2} \exp\left(\frac{1}{\theta}\right). \quad (11)$$

Then $\Xi'(\theta) = 0$ at

$$\theta_M = \frac{1}{2} - \frac{1}{2}\sqrt{1 - 4\theta_L} \quad \text{and} \quad \theta_m = \frac{1}{2} + \frac{1}{2}\sqrt{1 - 4\theta_L}, \quad (12)$$

where m stands for minimum and M for maximum, see Fig. 3.1.

In Fig. 3.1 we have $\theta_L = 0.17$ for the solid curve, $\theta_L = 0.15, 0.19, 0.21, 0.23$ for the dotted curves (from left to right), $\theta_L = 0.25$ for the dotted-dashed curve. Notice that when θ_L is smaller, the peak becomes larger. Notice that the intersection of each curve with the θ axis is the respective θ_L . Finally, notice that for the solid curve with $\theta_L = 0.17$ we mark, at the left of vertical axis, the regions where we have one or three solutions (with '1' or '3') of $\Xi(\theta) = \gamma d$. On the horizontal axis, we mark also the regions I, II, III where the corresponding $\theta_I, \theta_{II}, \theta_{III}$ would be. We notice that the first equation in (10) always has at least one root, which means that there is always a steady-state solution. In some cases, there are three different roots, and three different stationary solutions, related to the roots $\theta_I, \theta_{II}, \theta_{III}$ and notice that $\theta_L < \theta_I < \theta_M < \theta_{II} < \theta_m < \theta_{III}$.

FIGURE 3.1. Some $\Xi(\theta)$ versus θ .

3.2. Linear stability analysis of equilibria. We have found the stationary solutions for the Dirichlet condition. We will study time dependent solutions that are close to the stationary solution (8) to determine under which conditions $\varrho(x)$ is linearly stable.

Notice that when $\theta \approx \varrho$, using Taylor's formula, we can write

$$\exp(-1/\theta) \approx \exp(-1/\varrho)(1 + (\theta - \varrho)/\varrho^2). \quad (13)$$

Now using (13) on the first term of the RHS of (6.b), adding and subtracting ϱ_x and ϱ_t , recalling that $\varrho_t = 0$ and $\varrho(x=1)$ satisfies Eq. (7.b), we have that (6.b) becomes

$$\left. \frac{\partial(\theta - \varrho)}{\partial t} \right|_{x=1} \approx \gamma \exp(-1/\varrho)(\theta - \varrho)/\varrho^2 \Big|_{x=1} + \left. \frac{\partial(\theta - \varrho)}{\partial x} \right|_{x=1+}. \quad (14)$$

We now examine how the solution of the evolution problem behaves when we perturb the stationary solution around the solution ϱ . To do so, we define

$$\vartheta(x, t) := \theta(x, t) - \varrho(x). \quad (15)$$

Since we have assumed constant reservoir temperatures at the right boundary, we write the linear model for the perturbation, from Eqs. (14) and the heat equation, as

$$\begin{cases} \vartheta_t = \vartheta_{xx} & x \in (1, L), t > 0 \\ \vartheta_t|_{x=1} = \sigma \vartheta|_{x=1} + \vartheta_x|_{x=1+} & x \leq 1, t > 0 \end{cases} \quad (16)$$

where

$$\sigma = \sigma(\theta_o) := \gamma \exp(-1/\theta_o)/\theta_o^2. \quad (17)$$

for $\varrho(1) = \theta_o$. The homogeneous Dirichlet boundary and initial conditions are

$$\vartheta(L, t) = 0 \quad \text{and} \quad \vartheta(x, 0) = \vartheta_o(x). \quad (18)$$

3.3. Separation of variables. Equation (16) is the heat equation, and a classical approach to find its solution is separation of variables. We substitute the expression

$$\vartheta(x, t) := T(t)X(x), \quad (19)$$

into (16) to obtain for $t > 0$ and x in $(1, L)$

$$\frac{\dot{T}}{T}(t) = \frac{X''}{X}(x) = \lambda, \quad \text{or} \quad \dot{T} - \lambda T = 0 \quad \text{and} \quad X'' - \lambda X = 0, \quad (20)$$

where λ is a constant. So the temporal part has the form $T(t) = \exp(\lambda t)$, and therefore, we need to solve the following eigenvalue problem:

$$\begin{cases} X(x) = X(1) & x \in [0, 1) \\ \lambda X(x) = X''(x) & x \in (1, L) \\ \lambda X(1) = \sigma X(1) + X'(1+) \\ X(L) = 0. \end{cases} \quad (21)$$

The case $\lambda > 0$. Take $\lambda = \beta^2$, with $\beta \in \mathbb{R}^+$. Solving Eq. (21.b), we have

$$X(x) = A \exp(\beta x) + B \exp(-\beta x), \quad (22)$$

where A and B depend on β . Substitution of $X(x)$ from Eq. (22) into Eq. (21.d) shows that $B = -A \exp(2\beta L)$, and by substituting again in Eq. (21.c), we notice that for such $\beta \geq 0$ to exist, we need that

$$F(\beta) := \frac{\sigma - \beta^2 \sinh(\beta d)}{\beta \cosh(\beta d)} = \frac{\sigma - \beta^2}{\beta} \tanh(\beta d) = 1. \quad (23)$$

Using (17) and $F'(\beta)$ we notice that for (23) to be satisfied, we need that

$$\sigma(\theta_o)d = \gamma \exp(-1/\theta_o)d/\theta_o^2 > 1, \quad \text{so} \quad \gamma d \exp(-1/\theta_o) > \theta_o^2. \quad (24)$$

Manipulating (10) leads to $\gamma d \exp(-1/\theta_o) = \theta_o - \theta_L$. Comparing the latter equation with (24), we see that a root of β exists only if $0 > \theta_o^2 - \theta_o + \theta_L$ is satisfied. This requires that $\theta_o \in (\theta_M, \theta_m)$, given in Eqs. (12). In the Ξ vs. θ plot from Eq. (10) in Fig. 3.1, we see that when we have just one stationary solution, it lies out of (θ_M, θ_m) and therefore, we do not have any unstable mode; the solution must be stable.

We use the equality

$$\begin{aligned} \exp(\beta x) - \exp(\beta(2L - x)) &= \exp(\beta L) \left[\exp(\beta(x - L)) - \exp(\beta(L - x)) \right] \\ &= -2 \exp(\beta L) \sinh(\beta(L - x)), \end{aligned} \quad (25)$$

in Eq. (22), to compute the eigenfunction associated with the eigenvalue β as

$$X_o(x) := \begin{cases} C_o \sinh(\beta d), & x \in [0, 1] \\ C_o \sinh(\beta(L - x)), & x \in (1, L), \end{cases} \quad (26)$$

where $C_o := (\sinh^2(\beta d) + \sinh(2\beta d)/(2\beta) - d/2)^{-1}$ is a suitable constant to normalize the eigenfunction in the $L^2[0, L]$ space. A simple differentiation with respect to d shows that C_o is an increasing function of d , and because $d = 0$ implies $C_o = 0$, we have that $C_o > 0$ for $d > 0$.

The case $\lambda < 0$. We now look for negative eigenvalues. Take $\lambda = -\alpha^2$ and notice that α and $-\alpha$ give the same solution, so for convenience take $\alpha \in \mathbb{R}^-$. From Eq. (21.b), we have

$$-\alpha^2 X = X'', \quad (27)$$

it follows that $X(x)$ is a linear combination of sines and cosines with argument αx . But from Eq. (21.d), we have $X(L) = 0$, so it is better to choose

$$X(x) = A \sin(\alpha(L - x)), \quad (28)$$

where $A = A(\alpha)$ is a constant. By substituting (28) into Eq. (21.c) we get that $-\alpha$ must satisfy $-(\sigma + \alpha^2)A \sin(\alpha d) = -A\alpha \cos(\alpha d)$. Then, we are looking for $\alpha \in \mathbb{R}^-$ such that

$$\frac{\sigma + \alpha^2}{\alpha} = \frac{\cos(\alpha d)}{\sin(\alpha d)} = \cot(\alpha d). \quad (29)$$

Comparing the plot of both sides of (29), we see that there is a root α_n in each interval $-(n+1)\pi/d, -n\pi/d$ with $n \in \mathbb{N}$. The roots form a countable decreasing sequence of eigenvalues for our model. Each of these eigenvalues has an associated eigenfunction

$$X_n(x) := \begin{cases} C_n \sin(\alpha_n d), & x \in [0, 1] \\ C_n \sin(\alpha_n(L - x)), & x \in (1, L], \end{cases} \quad (30)$$

where $C_n := (\sin^2(\alpha_n d) - \sin(2\alpha_n d)/(2\alpha_n) + d/2)^{-1}$ are suitable positive normalizing constants for the eigenfunctions in the $L^2[0, L]$ space.

We have used the negative sign for α just for convenience. In this way, we only emphasize that the positive eigenvalue β corresponds to the unstable mode, while the negative eigenvalues α_n corresponds to the stable modes; if $\lambda < 0$ the solution (19) converges exponentially to zero. This arrangement is also convenient because it allows us to plot all the conditions in a single graph.

We can redefine the function in (23) as $F(y)$ below, using positive y for β and negative y for α , in this way:

$$F(y) := \begin{cases} (\sigma/y - y) \tanh(yd) & y > 0 \\ \sigma d & y = 0 \\ (\sigma/y + y) \tan(yd) & y < 0. \end{cases} \quad (31)$$

Now the roots of $F(y) = 1$ are all the eigenvalues; negative values of y correspond to eigenvalues $\lambda = -y^2$, and positive values of y correspond to eigenvalues $\lambda = y^2$. The plot of this function is in Fig. 3.2. From the limits

$$\lim_{y \rightarrow 0^-} (\sigma/y + y) \tan(yd) = \sigma d, \quad \text{and} \quad \lim_{y \rightarrow 0^+} (\sigma/y - y) \tanh(yd) = \sigma d, \quad (32)$$

we see that $F(y)$ is a continuous function at $y = 0$, for any σ or L . If we let σ and L move continuously so that σd becomes less than 1, then the positive eigenvalue no longer exists, because it becomes a negative eigenvalue. This is a very nice property.

It is possible also to show even more, the function $F(y) \in \mathcal{C}^\infty(\mathbb{R})$ except for $y = n\pi/d$, where is not defined. Although, its first derivative is continuous at $y = 0$.

Notice that for the unstable mode to exist we need $\sigma d > 1$, which is false when γd is less than the critical value $\sigma^* := 4 \exp(1/2)$; a bifurcation occurs right at this value! Because the height $F(y = 0)$ in Fig. 3.2 changes continuously for continuous variation of σ and d , we

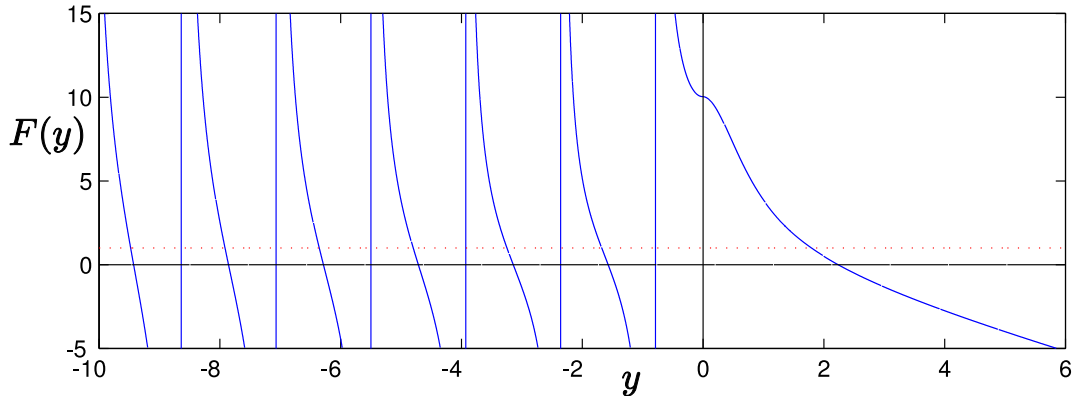


FIGURE 3.2. Positive and negative eigenvalues, $F(y) = 1$. There exists at most one positive eigenvalue.

have that the bifurcation from one stable solution to the three steady-state solutions (one unstable and two stable) is continuous dependent in such parameters.

3.4. Evolution of the linearized model. The solution $\vartheta(x, t)$ is obtained by superposition of all modes given by Eq. (19). We saw that we have to proceed differently for eigenvalues $\lambda \leq 0$ and $\lambda > 0$. Therefore, with the superposition of the solutions in (26) and (30), we have that the solution of the linearized model is

$$\vartheta(x, t) = A_o \exp(\beta^2 t) \sinh(\beta(L - x)) + \sum_{n \in \mathbb{N}} A_n \exp(-\alpha_n^2 t) \sin(\alpha_n(L - x)), \quad (33)$$

where the coefficients $A_n := \langle \vartheta_o, X_n \rangle$, $\forall n \in \mathbb{N}$ are obtained by comparing (33) at time zero with the initial condition $\vartheta_o(x)$. This superposition is all that we need due the completeness and orthonormality of the eigenfunctions in the region $[0, L]$, the formal arguments are contained in the thesis (Castañeda, 2010).

Remark: Notice that there exists one and only one positive eigenvalue when $\theta_o \in (\theta_M, \theta_m)$, with θ_M, θ_m given by (12). When $1 - 4\theta_L < 0$, there is no unstable equilibrium, and the temperature of the reservoir goes to the (unique) stationary solution.

4. NUMERICAL METHOD

In this section we discuss a finite difference scheme that we used for the nonlinear problem (6), with $\mathcal{E} = 1$. We implement the Crank-Nicolson method (CN). For the heat equation, in the domain $x \in [1, L]$ it would be:

$$-\frac{\mu}{2}v_{m+1}^{n+1} + (1 + \mu)v_m^{n+1} - \frac{\mu}{2}v_{m-1}^{n+1} = \frac{\mu}{2}v_{m+1}^n + (1 - \mu)v_m^n + \frac{\mu}{2}v_{m-1}^n, \quad (34)$$

where $v_m^n = v(mh + 1, nk)$ is the discrete solution (then v_o^n represents $v(1, nk)$), $\mu := k/h^2$, h is the grid spacing and k is the time interval. The CN method is of order $\mathcal{O}(h^2, k^2)$, and it is unconditionally stable.

The right boundary condition is governed by $v_M^{n+1} = v_M^n$, where $M := (L - 1)/h$. In order to discretize the left boundary, $x = 1$, where $\theta_t = \gamma \exp(-1/\theta) + \theta_x$, we recall that one way of deriving the discretization of CN method utilizes an auxiliary grid point between two step

times, namely $(1 + mh, (n + \frac{1}{2})k)$. For the sake of consistency we have to expand the time derivatives at the boundary around the auxiliary point $(1, (n + \frac{1}{2})k)$. Notice that

$$\begin{aligned} \theta(1, (n + 1/2 \pm 1/2)k) &= \theta(1, (n + 1/2)k) \pm 1/2\theta_t(1, (n + 1/2)k) \\ &\quad + (k^2/8)\theta_{tt}(1, (n + 1/2)k) + \mathcal{O}(k^3). \end{aligned} \quad (35)$$

By subtracting the (+) equation from the (-) equation in (35), and dividing by k , we find

$$\theta_t(1, (n + 1/2)k) = \frac{\theta(1, (n + 1)k) - \theta(1, nk)}{k} + \mathcal{O}(k^2). \quad (36)$$

We do something similar for the spatial derivative, but in this case, we use spatial average at two neighboring grid points by adding both Eqs. (35), the (-) and the (+), for θ_x instead of θ . Notice that $\theta_x(1, \cdot) = [\theta(1 + h, \cdot) - \theta(1, \cdot)]/h + \mathcal{O}(h)$, then

$$\begin{aligned} \theta_x(1, (n + 1/2)k) &= \frac{1}{2} \left[\frac{\theta(1 + h, (n + 1)k) - \theta(1, (n + 1)k)}{h} \right. \\ &\quad \left. + \frac{\theta(1 + h, nk) - \theta(1, nk)}{h} \right] + \mathcal{O}(h, k^2). \end{aligned} \quad (37)$$

Finally we can write

$$\exp\left(\frac{-1}{\theta(1, (n + 1/2)k)}\right) = \frac{1}{2} \left[\exp\left(\frac{-1}{\theta(1, (n + 1)k)}\right) + \exp\left(\frac{-1}{\theta(1, nk)}\right) \right] + \mathcal{O}(k^2). \quad (38)$$

From these approximations, we get the final form for the boundary condition

$$\left(1 + \frac{\lambda}{2}\right)v_o^{n+1} - \frac{\lambda}{2}v_1^{n+1} - \frac{k\gamma}{2}\exp\left(\frac{-1}{v_o^{n+1}}\right) = \left(1 - \frac{\lambda}{2}\right)v_o^n + \frac{\lambda}{2}v_1^n + \frac{k\gamma}{2}\exp\left(\frac{-1}{v_o^n}\right). \quad (39)$$

Although this boundary scheme is of first order in space in comparison to the former base scheme of second order, this is not a problem, because the stability and convergence of the overall results are not impaired in the simulations. Moreover, the accuracy of the overall scheme is not altered; it is second order in space and time.

4.1. Implementation of the numerical method. Let $h = (L - 1)/M$ be the size of the spatial grid and $M + 1$ the number of spatial nodes of the numerical domain. Let $v^n := (v_o^n, v_1^n, \dots, v_M^n)^T$. We write the CN method as

$$Av^{n+1} - U(v^{n+1}) = Bv^n + U(v^n), \quad \text{where } U(v^n) := \left(\frac{k\gamma}{2}\exp\left(-\frac{1}{v_o^n}\right), 0, \dots, 0\right)^T \quad (40)$$

and

$$A := \begin{pmatrix} 1 + \frac{\lambda}{2} & -\frac{\lambda}{2} & 0 & & & \\ -\frac{\mu}{2} & 1 + \mu & -\frac{\mu}{2} & & & \\ & \ddots & \ddots & \ddots & & \\ & & -\frac{\mu}{2} & 1 + \mu & -\frac{\mu}{2} & \\ & & 0 & 0 & 1 & \end{pmatrix}, \quad B := \begin{pmatrix} 1 - \frac{\lambda}{2} & \frac{\lambda}{2} & 0 & & & \\ \frac{\mu}{2} & 1 - \mu & \frac{\mu}{2} & & & \\ & \ddots & \ddots & \ddots & & \\ & & \frac{\mu}{2} & 1 - \mu & \frac{\mu}{2} & \\ & & 0 & 0 & 1 & \end{pmatrix}.$$

We want to solve each step of the implementation by Newton's method. Let be $\omega^o := v^n$ and we will iterate with $\omega^{l+1} := \omega^l + d^l$, where d^l is a vector that corrects the last prediction ω^l . In this way we see how v^{n+1} is obtained from ω^l .

We are looking for d^l such that ω^{l+1} solves (40.a) instead of v^{n+1} . Set $K := Bv^n + U(v^n)$, that will remain fixed for a given n . Assuming d_o^l small, we use Taylor's formula to express

$$\exp\left(\frac{-1}{\omega_o^{l+1}}\right) = \exp\left(\frac{-1}{\omega_o^l + d_o^l}\right) = \exp\left(\frac{-1}{\omega_o^l}\right) \left(1 + \frac{d_o^l}{(\omega_o^l)^2}\right) + \mathcal{O}((d_o^l)^2), \quad (41)$$

so, we have the iterative equation

$$Ad^l + U(\omega^l) \frac{d_o^l}{(\omega_o^l)^2} = K - A\omega^l + U(\omega^l). \quad (42)$$

To solve this equation, let $M_l := -A\omega^l + U(\omega^l)$ and

$$\Lambda := \begin{pmatrix} \alpha_l & -\frac{\lambda}{2} & 0 & & \\ -\frac{\mu}{2} & 1 + \mu & -\frac{\mu}{2} & & \\ & \ddots & \ddots & \ddots & \\ & & -\frac{\mu}{2} & 1 + \mu & -\frac{\mu}{2} \\ & & 0 & 0 & 1 \end{pmatrix}, \quad (43)$$

where $\alpha_l = 1 + \frac{\lambda}{2} - \frac{k\gamma}{2(\omega_o^l)^2} \exp\left(-\frac{1}{\omega_o^l}\right)$. Then, Eq. (42) is $d^l = \Lambda^{-1}(K + M_l)$. At the start of each iteration, we take $\omega^{l+1} = \omega^l + d^l$ and update M_l and Λ at $\mathcal{O}(1)$ cost. However, we need to solve a linear system with Λ in each iteration, which is expensive.

Notice that the matrices A and Λ differ only in the first diagonal entry, which changes at each step of Newton's method. Note that making an UL factorization for the A matrix and the Λ matrix gives the same U matrix. However, the L matrix differs only in the first diagonal entry, the α_l of Eq. (43). In short

$$\Lambda(l) = UL(l), \quad (44)$$

which means that Λ and L depend upon the iteration step. Then finding the inverse of U , once and for all, outside the iterative solver, improves the solver, and equation (42) becomes

$$L(l)d^l = U^{-1}(K + M_l). \quad (45)$$

Comparing (42) with (45), we see that we have replaced the resolution of a tridiagonal system, in each step of the iterative solver, by the resolution of a lower bidiagonal system. This algorithm improves the machine time by almost 50%.

4.2. Numerical results. Recall that in Sec. 2 we had $\gamma = 7 \times 10^8$. Using such large values of γ in the numerical method leads to slow convergence: in the nonlinear part, Eq. (39), the α_l coefficient in the solver increases and the solver requires a small step time k in order to guarantee convergence. Nevertheless, we are interested in simulating situations in the model containing three steady-state solutions and see the qualitative behavior of its solutions. We do so for relatively small values of γ .

Even using a coarse mesh, we obtain good convergence to both stable stationary solutions. For $k = 0.2$ and $h = 0.01$ we get an error no larger than 10^{-2} in comparison to the actual θ_I and θ_{III} values.

A good example of this behavior is the following. We set $\gamma = 1/4$, the reservoir temperature $\theta_L = 0.2$ and $L = 10$. For these parameters, the stationary left temperatures are $\theta_I \approx$

0.22803135, $\theta_{II} \approx 0.47920158$ and $\theta_{III} \approx 1.12500985$. Furthermore, we set the grid numbers $h = 0.05$ and $k = 0.2$, and the initial condition

$$u_o(x) = \frac{(\theta_L - \theta_i)x + \theta_i L - \theta_L}{L - 1} + 0.4095 \sin(0.6(L - x)) + 0.5905 \sin(0.4(L - x)), \quad (46)$$

where $\theta_i = 0.4792015876$. The results of simulation for the unstable stationary solution agree with our intuition: the evolution of the numerical solution approaches the unstable equilibrium solution in a very short time, $t \approx 30$. It remains close to that solution for long time: it diverges only for $t > 800$, and approaches a stable stationary solution around $t \approx 1850$. Notice that using a bisection method we can find initial conditions that remain close to the unstable solution for times as long as we please. This result is plotted at some times on Fig. 4.1 for CN. In this figure we also show results for the Backward Euler method with central differentiation (BE). Refining the grid numbers will show that the convergence has to be, in both cases, to $\varrho_I(x)$.

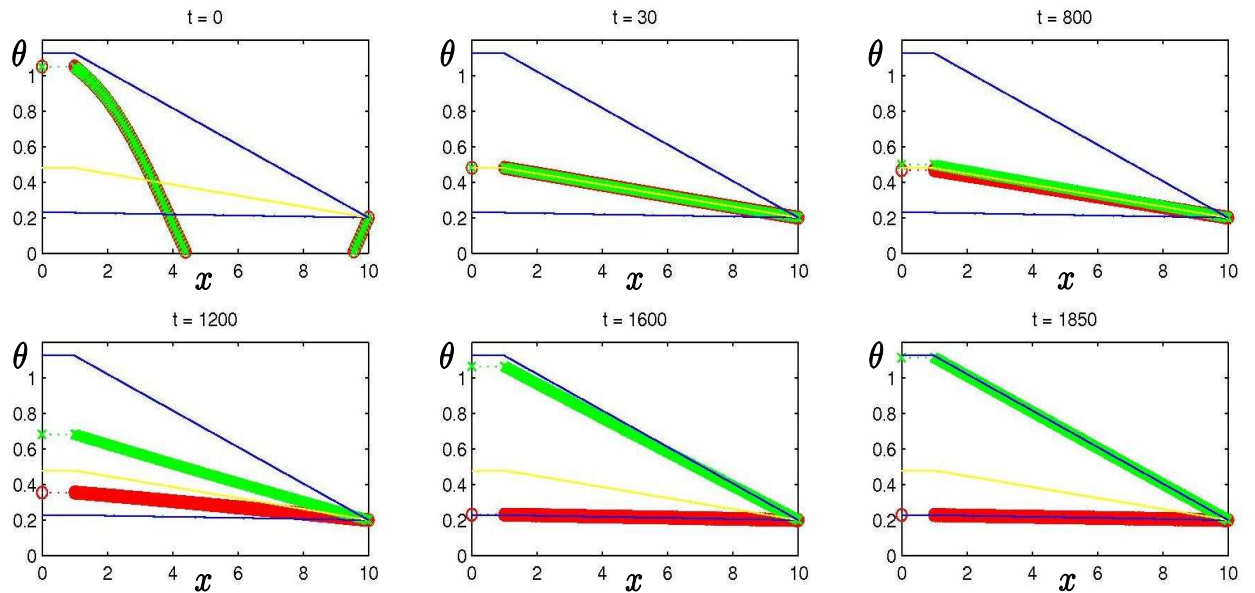


FIGURE 4.1. The initial condition, for time $t = 0$, given in (46) is plotted on the top left. We plot with dark circles the CN method and with light crosses the BE method, the three “linear” plots are the three stationary solutions. For times closer to $t = 30$ the solution obtained by both methods approximate asymptotically the unstable solution. Both solutions remain close to it until $t = 800$. The bifurcation starts leading CN to $\varrho_I(x)$ at $t = 1600$ and BE to $\varrho_{III}(x)$ at $t = 1850$.

Several simulations show that the behavior of any solution of the nonlinear model always has a fast convergence to an almost linear profile, from which the solution will be driven to one of the stable stationary solutions. Such separation between trajectories that converge to $\varrho_I(x)$ from those converging to $\varrho_{III}(x)$ appears to occur at a value $\theta(1, t)$ comparable to θ_{II} .

5. CONCLUDING REMARKS

The numerical simulation showed that the stable modes, related to negative eigenvalue λ , decrease very fast; therefore a model with linear profiles is a good global approximation of the solution for the complete model for large times. This model is analyzed in (Castañeda, 2010).

Furthermore, the resulting equilibrium θ_{III} related with the ignition, is prevalent because of the typically large values of γ , which has to be of order 7.0×10^8 . If we recall the condition given in Eq. (10) we note that for the existence of stationary solution, we need θ_o to be of order of γ times d , a huge nondimensional temperature. By comparison we note that $E/R \approx 2 \times 10^4$ K, and then T_{III} , the temperature related to the nondimensional combustion value θ_{III} , is of order $d \times 10^{13}$ Kelvin's degrees! Certainly this range is unphysical; this problem arises from the limitations of this model, *i.e.*, the heat loss is only one-dimensional. Other geometries will correct this limitation.

The two ideal cases in order to get combustion as a final state are: initial conditions with large amounts of coke and oxygen in a single steady-state equilibrium model, which is related to combustion or, for the full three steady-state model, temperatures at the reaction region higher than T_{II} . Perhaps, the dissipation of heat will not extinguish the combustion since we have neglected the consumption of coke and oxygen, it is clear that the reaction remains active forever, generating heat all the time. However, in the physical situation the concentrations of the reactants will decrease, but in order to maintain the combustion rate, we need to maintain them with $\gamma d > \Xi(\theta(1, t))$ for $\theta(1, t) \geq \theta_M$ or $\Xi(\theta(1, t)) > \Xi(\theta_m)$ otherwise, see Fig. 1.

From the numerical simulation, we can see that the assumption of "eternal" fuel is not so extreme, because for long times the reaction starts slowly far away from the equilibrium burning small quantities of coke and oxygen, and then ignition will occur for large initial concentrations of C and O_2 .

Finally, based on this model we cannot determine when or where a combustion can exist, only when it cannot. For small perturbations of a linear initial profile with $\theta(1, 0) < \theta_{II}$, we are in the extinction region. Here the conclusions are valid.

We have used some special values to estimate γ and compared these results against other values; using different activation energies and prefactors given in (Rybak, 1988), we set the prefactor $(Ac_o) = 2.22 \times 10^6 s^{-1}$ that is in the range $1.97 \times 10^5 s^{-1}$, $3.62 \times 10^7 s^{-1}$. Therefore for a reservoir temperature of 300 K will find that $T_M = 309.24$ K and $T_m = 1.8704 \times 10^4$ K, the temperatures related to θ_M , θ_m in Eq. (12). Thus the unstable temperature will exist and vary between these values only when the reservoir has a size for the dimensional d from 3.82×10^{-8} m to 1.9×10^{15} m. An example is for a 10 Km reservoir which would give $T_{II} = 560,88$ K so the temperature at the boundary has to exceed this value T_{II} in order to ignite. For smaller reservoirs this temperature would be larger, and the domain of extinction will grow until T_{II} reach the T_m value, which is the limit to the model with only one steady-state solution.

Acknowledgments. The material presented here is supported by the doctoral scholarship from CAPES - PEC-PG.

REFERENCES

- [1] S.A. ABU-KHAMSIN, W.E. BRIGHAM AND H.J. RAMEY (1988) “Reaction kinetics of fuel formation for in-situ combustion”, *SPE Reservoir Engineering* **3:4**: 1308–1316.
- [2] J. BRUINING AND D. MARCHESIN (2008) “Spontaneous ignition in porous media at long times”, ECMOR XI. 8-11 Sept., 11th European Conference on the Mathematics of Oil Recovery. Bergen, Norway.
- [3] P. CASTAÑEDA (2010) *Chemical reactors in porous media*. (Defended on 4 January 2010.) [<http://www.preprint.impa.br/>] Doctoral thesis, IMPA/Brasil.
- [4] W. RYBAK (1988) “Intrinsic reactivity of petroleum coke under ignition conditions”, *Fuel* **67**: 1696–1702.
- [5] R.J. TYLER (1985) “Intrinsic reactivity of petroleum coke to oxygen”, *Fuel* **65**: 235–240.

PABLO CASTAÑEDA

DAN MARCHESIN

INSTITUTO NACIONAL DE MATEMÁTICA PURA E APLICADA

ESTRADA DONA CASTORINA, 110

RIO DE JANEIRO, RJ 22460-320, BRAZIL

E-mail address: castaneda@impa.br

E-mail address: marchesin@impa.br

JOHANNES BRUINING

SECTION GEOENGINEERING, DELFT UNIVERSITY OF TECHNOLOGY

P.O. BOX 5048, 2600 GA, DELFT, THE NETHERLANDS

E-mail address: J.Bruining@tudelft.nl